

# Scattering searches for dark matter in subhalos: neutron stars, cosmic rays, and old rocks

Joseph Bramante,<sup>1,2,\*</sup> Bradley J. Kavanagh,<sup>3,†</sup> and Nirmal Raj<sup>4,‡</sup>

<sup>1</sup>*The Arthur B. McDonald Canadian Astroparticle Physics Research Institute,  
Department of Physics, Engineering Physics, and Astronomy,  
Queen's University, Kingston, Ontario, K7L 2S8, Canada*

<sup>2</sup>*Perimeter Institute for Theoretical Physics, Waterloo, Ontario, N2L 2Y5, Canada*

<sup>3</sup>*Instituto de Física de Cantabria (IFCA, UC-CSIC),  
Av. de Los Castros s/n, 39005 Santander, Spain*

<sup>4</sup>*TRIUMF, 4004 Wesbrook Mall, Vancouver, BC V6T 2A3, Canada*

(Dated: September 13, 2021)

In many cosmologies dark matter clusters on sub-kiloparsec scales and forms compact subhalos, in which the majority of Galactic dark matter could reside. Null results in direct detection experiments since their advent four decades ago could then be the result of extremely rare encounters between the Earth and these subhalos. We investigate alternative and promising means to identify subhalo dark matter interacting with Standard Model particles: (1) subhalo collisions with old neutron stars can transfer kinetic energy and brighten the latter to luminosities within the reach of imminent infrared, optical, and ultraviolet telescopes; we identify new detection strategies involving single-star measurements and Galactic disk surveys, and obtain the first bounds on self-interacting dark matter in subhalos from the coldest known pulsar, PSR J2144–3933, (2) subhalo dark matter scattering with cosmic rays results in detectable effects, (3) historic Earth-subhalo encounters can leave dark matter tracks in paleolithic minerals deep underground. These searches could discover dark matter subhalos weighing between gigaton and solar masses, with corresponding dark matter cross sections and masses spanning tens of orders of magnitude.

**Introduction.** The enigma of dark matter persists [1]. In the hope that its microscopic properties will be revealed through its scattering and annihilation into Standard Model (SM) states, extensive experimental efforts are underway to detect it [2–4]. Both direct and indirect dark matter (DM) searches often assume that DM is smoothly distributed over the Galactic halo. However, cold DM is expected to form subhalo structures down to Earth-mass scales ( $\sim 10^{-6} M_{\odot}$ ) [5–7]. Such substructure should persist on length scales below a kiloparsec if small DM halos remain un-disrupted during hierarchical clustering, as suggested by  $N$ -body simulations [8–10]. Furthermore, in many cosmological scenarios the small-scale power is enhanced – via, e.g., an early matter-dominated era or DM self-interactions augmenting primordial density perturbations – resulting in large fractions of DM surviving in subhalos [11–18].

It is known that for annihilating DM, subhalos could boost Galactic indirect detection fluxes, since the annihilation rate scales as the DM density squared [19–23]. Due attention has been paid to annihilation signals for this reason, but it may be that DM only reveals its interactions with SM states via scattering processes, such as when it is asymmetric [24] or its annihilation is  $p$ -wave-dominated [25–27]. Should the interacting component of DM reside in subhalos, direct detection experiments [28–30] may have observed no conclusive signal simply be-

cause the Earth has yet to encounter a subhalo since their inception. Thus other, novel probes of DM scattering are needed; in this *Letter* we outline three strategies.

The first is to observe heating of old, nearby neutron stars (NSs) by subhalo DM. These NSs will travel through subhalos and capture constituent DM particles, in a process that transfers DM kinetic energy of order the DM mass, because of the steep gravitational potential around NSs. This method was first proposed to detect smooth halo DM [31], which would result in infrared emission from NSs observable by upcoming telescopes, and is currently an active area of research [32–51]. Here we show that subhalo DM can impart larger NS luminosities than diffuse DM, bringing imminent optical and ultraviolet observations into play. Moreover, for DM with strong self-interactions, we show that due to enhanced accretion there is parameter space *already* constrained by observations of the coldest known NS, PSR J2144–3933 [52]. All in all, NS luminosity searches can probe gigaton to solar mass subhalos, for DM-nucleon cross sections as low as  $10^{-45} \text{ cm}^2$ .

Two other strategies to detect distant DM subhalos involve terrestrial probes that do not rely on Earth's spatial position or the usual years-long runtime of terrestrial experiments. Specifically, encounters of subhalo DM with Galactic cosmic rays and with geological minerals deep underground can be discerned in several ways discussed below. Under the assumption of a smooth halo, cosmic rays and minerals have already been utilized to constrain strongly-interacting DM [53–59]; here we will use these to set limits on DM subhalo masses and radii.

Current constraints on subhalos come from gravita-

---

\* joseph.bramante@queensu.ca

† kavanagh@ifca.unican.es

‡ nraj@triumf.ca

tional microlensing surveys, applicable for asteroid to solar mass subhalos with sizes ranging up to stellar radii [60, 61], and additional gravitational probes include pulsar timing arrays [62] and accretion glows in molecular clouds [63]. Direct detection of clustered DM up to the Planck mass was studied in Ref. [17], of higher mass composite DM in Refs. [64–70], and similar sensitivities with ancient minerals in Refs. [71–73]. Asteroid-mass subhalos colliding with stars were studied in Ref. [74], assuming geometric cross sections. We do not make this assumption and treat more general microscopic DM cross sections. Finally, DM substructure could impact direct detection experiments [75–77] and the biosphere [78].

**Neutron star heating and cooling.** In this study we consider subhalos of uniform density of mass  $M$  and maximum radius  $R_{\text{sh}}$ ; other density profiles are expected to impact these results at the  $\mathcal{O}(1)$  level. For simplicity we assume all NSs are of the same mass  $M_{\text{NS}}$  and radius  $R_{\text{NS}}$ , with benchmark parameters

$$M_{\text{NS}} = 1.5 M_{\odot}, \quad R_{\text{NS}} = 10 \text{ km}. \quad (1)$$

The rate of NS-subhalo encounters for a single NS with  $M_{\text{NS}} \gg M$  is then given by [79, 80]:

$$\Gamma_{\text{meet}}(r) = 4\sqrt{\pi} f_{\chi} \frac{\rho_{\chi}(r)}{M} (R_{\text{sh}} + R_{\text{NS}})^2 \sigma_v(r) \times \left( 1 + \frac{GM_{\text{NS}}}{2\sigma_v^2(r)(R_{\text{sh}} + R_{\text{NS}})} \right), \quad (2)$$

where  $\rho_{\chi}(r)$  and  $\sigma_v(r)$  are the DM density and speed dispersion at Galactic position  $r$ . Here we have averaged the rate over the relative velocity  $v_{\text{rel}}$  of the encounters, which we assume to follow a Maxwell-Boltzmann distribution with dispersion  $\sigma_{v_{\text{rel}}}(r) = \sqrt{2}\sigma_v$  [81, Problem 8.8]. For the solar position  $r_{\odot} = 8.3$  kpc, we have  $\rho_{\odot} = 0.4$  GeV/cm<sup>3</sup> and  $\sigma_v = 156$  km/s [82], and for  $R_{\text{sh}} \ll R_{\text{NS}}$ :

$$\Gamma_{\text{meet}}(r_{\odot}) = \frac{f_{\chi}}{1.9 \text{ Gyr}} \left( \frac{10^{-15} M_{\odot}}{M} \right). \quad (3)$$

For concreteness, in our numerical results we fix the fraction of DM in subhalos as  $f_{\chi} = 1$ .

Assuming that all of the incident DM flux in the subhalo is captured by the NS, the DM kinetic energy deposited in the NS after subhalo passage is

$$E_{\text{meet}} = zM \min \left[ 1, \left( \frac{R_{\text{co}}}{R_{\text{sh}}} \right)^2 \right], \quad (4)$$

where the blueshift of DM falling into the neutron star increases the DM kinetic energy according to

$$1 + z = \frac{1}{\sqrt{1 - 2GM_{\text{NS}}/R_{\text{NS}}}} = 1.34, \quad (5)$$

and the effective gravitational collection radius  $R_{\text{co}}$  of the neutron star is:

$$R_{\text{co}} = \left( \frac{v_{\text{esc}}}{\langle v_{\text{rel}} \rangle} \right)^{\ell} R_{\text{NS}} (1 + z), \quad (6)$$

where  $\langle v_{\text{rel}} \rangle \simeq 350$  km/s is the average subhalo-NS relative speed,  $\ell = 1$  if the DM in the subhalo is effectively collisionless [83], and  $\ell = 2$  for DM that behaves like a fluid, in which case  $R_{\text{co}}$  will be the Bondi radius [84–87]. The latter expression assumes that the sound speed in the subhalo does not exceed the NS-subhalo relative velocity. In Eq. (6), the escape velocity at the NS surface is  $v_{\text{esc}} = \sqrt{2GM_{\text{NS}}/R_{\text{NS}}}$ , and the  $1 + z$  factor accounts for the apparent NS radius to distant observers. DM in subhalos will heat an NS from internal temperature  $\tilde{T}_{\text{cold}}$  to  $\tilde{T}_{\text{hot}}$  given by

$$\int_{\tilde{T}_{\text{cold}}}^{\tilde{T}_{\text{hot}}} d\tilde{T} c_V(\tilde{T}) = E_{\text{meet}}. \quad (7)$$

Here and throughout this paper, the tilde denotes temperatures measured by a distant observer:  $\tilde{T} \equiv T/(1+z)$ , where  $T$  is the NS local core temperature.

The NS heat capacity  $c_V$  depends sensitively on the superfluid and superconducting properties of NS nucleons. It has long been recognized that nucleons could indeed form Cooper pairs in NS cores with an MeV energy gap, corresponding to a critical temperature  $T_c \simeq 10^{10}$  K [88–90]. Observational fits to cooling curves support this hypothesis [91]. The heat capacity of degenerate matter is set by particle-hole excitations close to the Fermi surface, thus the energy gap exponentially suppresses the nucleon contribution to the heat capacity for NS temperatures  $\ll T_c$ , the temperature zone we are interested in. Hence our NS heat capacity is set by the contribution from degenerate electrons (whose pairing-up critical temperature is  $< 100$  K), and is given by

$$c_V(\tilde{T}) = 4.8 \times 10^{26} \text{ J/K} \left( \frac{\tilde{T}}{10^4 \text{ K}} \right) = 2.7 \times 10^{-21} M_{\odot}/\text{K} \left( \frac{\tilde{T}}{10^4 \text{ K}} \right). \quad (8)$$

Here we have used analytic fits for the electronic  $c_V$  provided in Ref. [92]. In general we expect  $\mathcal{O}(10\%)$  variations to the above arising from the choice of the equation of state (EoS) for NS core matter and of the NS mass-radius configuration; in this work we use Eq. (8).

Putting Eqs. (7) and (8) together, we obtain

$$\left( \frac{\tilde{T}_{\text{hot}}}{10^4 \text{ K}} \right)^2 = \left( \frac{\tilde{T}_{\text{cold}}}{10^4 \text{ K}} \right)^2 + \frac{E_{\text{meet}}}{6.2 \times 10^{-18} M_{\odot}}. \quad (9)$$

Between subhalo encounters the NS cools by emitting photons from its surface and neutrinos from its interior; the latter mode is sub-dominant for  $\tilde{T} \lesssim 10^8$  K, which corresponds to a surface temperature (generally different from  $\tilde{T}$  due to an insulating “envelope” on the NS) of  $\tilde{T}_s \lesssim 10^6$  K. The time for the NS to cool to  $\tilde{T}_{\text{cool}}$ , in a process that is insensitive to the starting temperature, is given by [93]

$$t_{\text{cool}}(\tilde{T}_9)/\text{yr} = \begin{cases} t_{\text{env}} = s_1^{-k} q^{-\gamma} [(1 + (s_1/q)^k \tilde{T}_9^{2-n})^{-\gamma/k} - 1], & \tilde{T}_{\text{cool}} > \tilde{T}_{\text{env}}, \\ t_{\text{env}} + (3s_2)^{-1} (\tilde{T}_9^{-2} - \tilde{T}_{\text{env}}^{-2}), & \tilde{T}_{\text{cool}} \leq \tilde{T}_{\text{env}}, \end{cases} \quad (10)$$

where  $\tilde{T}_9 = \tilde{T}_{\text{cool}}/(10^9 \text{ K})$ ,  $q = 2.75 \times 10^{-2}$ ,  $s_1 = 8.88 \times 10^{-6}$ ,  $s_2 = 8.35 \times 10^4$ ,  $k = (n-2)/(n-\alpha)$  and  $\gamma = (2-\alpha)/(n-\alpha)$  with  $\alpha = 2.2$  and  $n = 8$ . The temperature  $\tilde{T}_{\text{env}} \simeq 4000 \text{ K}$  corresponds to the time after which the surface and internal NS temperatures equalize due to the thinning of the crustal outer envelope. See Supplementary Material for notes on Eq. (10).

**Frequent NS encounters.** If subhalos heat NSs often enough, the NSs will maintain a steady-state temperature. Specifically, if the NS cooling time  $t_{\text{cool}}(\tilde{T}_s)$  exceeds the timescale between subhalo encounters  $t_{\text{meet}} = \Gamma_{\text{meet}}^{-1}$ , and if the encounters are energetic enough to impart temperatures  $> \tilde{T}_s$ , the NS will maintain a temperature of at least  $\tilde{T}_s$ . To find this temperature in terms of subhalo parameters, we set  $\tilde{T}_{\text{hot}}^2 = 2\tilde{T}_{\text{cold}}^2$  in Eq. (9) to estimate the  $E_{\text{meet}}^T$  required to attain a steady-state temperature in the vicinity of  $\tilde{T}_{\text{cold}}$ , which we call  $E_{\text{meet}}^T$ . Then for a given subhalo radius and NS accretion rate,  $E_{\text{meet}}^T$  corresponds to some  $M$  in Eq. (4), which also implies a unique  $t_{\text{meet}}$  in Eq. (2).

In Fig. 1 we plot as a function of  $\tilde{T}_s$  (corresponding to the  $E_{\text{meet}}^T$  in the top x-axis) both  $t_{\text{cool}}$  and  $t_{\text{meet}}(r_\odot)$  for various  $R_{\text{sh}}$ . The condition  $t_{\text{meet}} < t_{\text{cool}}$  then defines the NS temperatures for which a steady state scenario is possible. It can be seen that the subhalo encounter timescale does not exceed the cooling time for  $\tilde{T}_s \lesssim 3000 \text{ K}$  in the limits where the subhalo is much smaller or much larger than the NS, whereas for  $R_{\text{sh}}$  comparable to  $R_{\text{NS}}$  the condition could produce hotter NSs. This follows from Eqs. (2) and (4). For  $R_{\text{sh}} \ll R_{\text{NS}}$  both  $t_{\text{meet}}$  and  $E_{\text{meet}} \propto M$ , and for  $R_{\text{sh}} \gg R_{\text{NS}}$  both  $t_{\text{meet}}$  and  $E_{\text{meet}} \propto MR_{\text{sh}}^{-2}$ , thus the  $t_{\text{meet}}$  vs  $E_{\text{meet}}^T$  curves are co-incident in these limits. For intermediate  $R_{\text{sh}}$  the Sommerfeld enhancement factors for  $\Gamma_{\text{meet}}$  and  $E_{\text{meet}}$  differ in such a way that greater energies can be deposited in less frequent encounters.

The coldest NS observed, PSR J2144–3933, has a temperature upper limit of  $2.9 \times 10^4 \text{ K}$  for our benchmark NS [52], whereas our largest achievable steady-state temperature is  $\tilde{T}_s < 2 \times 10^4 \text{ K}$  (for  $R_{\text{sh}} = 10^4 \text{ km}$ ), for DM that accretes onto NSs in the collisionless regime, *i.e.*  $\ell = 1$  in Eq. (6). In the top panel of Fig. 2 we show, in the space of  $M$  vs  $R_{\text{sh}}$ , the subhalo parameters that can be explored in the future by measuring  $\tilde{T}_s$  down to 1000 K using upcoming infrared telescopes like JWST, ELT and TMT, within achievable times [31, 32]. This region is bounded on the left by a black-dashed contour of  $\tilde{T}_{\text{hot}} = 1000 \text{ K}$  (obtained from Eq. (9) for  $\tilde{T}_{\text{cold}} \ll \tilde{T}_{\text{hot}}$ ), and on the right by a black-dashed contour of  $t_{\text{meet}} = t_{\text{cool}}(1000 \text{ K}) = 1.2 \times 10^7 \text{ yr}$ , and would be excluded if an NS at  $r = r_\odot$  is measured to be below

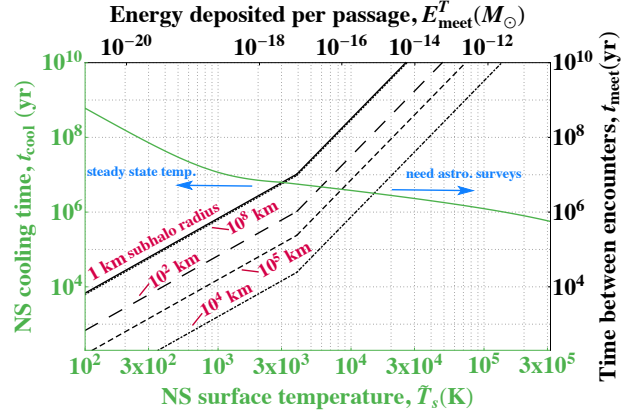


FIG. 1. Regions showing “frequent” vs “infrequent” NS-subhalo encounters, requiring different observational strategies. **Green:** Neutron star cooling time as a function of surface temperature  $\tilde{T}_s$ , assuming superfluid nucleons. **Black:** The time between encounters at the Solar position for various subhalo radii, as a function of the DM kinetic energy deposited in NSs per encounter, obtained from Eqs. (2) and (4). The top x-axis shows energies required to maintain corresponding steady-state  $\tilde{T}_s$  values in the bottom x-axis. To the left of black-green intersections, observations of a single NS with indicated temperatures would probe corresponding subhalo masses and radii. To the right, astronomical surveys are required to find NS ensembles exceeding indicated temperatures. See text for further details.

1000 K. (For a similar region corresponding to  $10^4 \text{ K}$ , see Supplementary Material.)

On the other hand, if DM has substantial self-interactions then PSR J2144–3933 *already* places a strong bound on subhalo DM. In this case we consider fluid accretion of the DM onto NSs, especially relevant for theories of dissipative and strongly self-interacting DM [94–98], for which DM will have a sizable sound speed (much like the interstellar medium), especially if collected into dense subhalos. The effective DM collection radius of the NS will now be enhanced by another factor of  $v_{\text{esc}}/\langle v_{\text{rel}} \rangle$  (*i.e.*  $\ell = 2$  in Eq. (6)) [84–87], and in a large parametric region Bondi accretion imparts enough energy for all NSs near Earth to have temperatures in excess of  $2.9 \times 10^4 \text{ K}$ . Thus in Fig. 2, the orange region is already constrained by the  $\tilde{T}_s \lesssim 3 \times 10^4 \text{ K}$  bound on PSR J2144–3933’s temperature [52]. Additional bounds may be obtained for subhalo DM with strong self-interactions from *e.g.* the Bullet Cluster – these will depend on a detailed simulation of subhalo collisions, and the specific self-interacting DM model [99].

The regions just discussed may be probed so long as the dynamics of the DM-NS scattering process lead to cap-

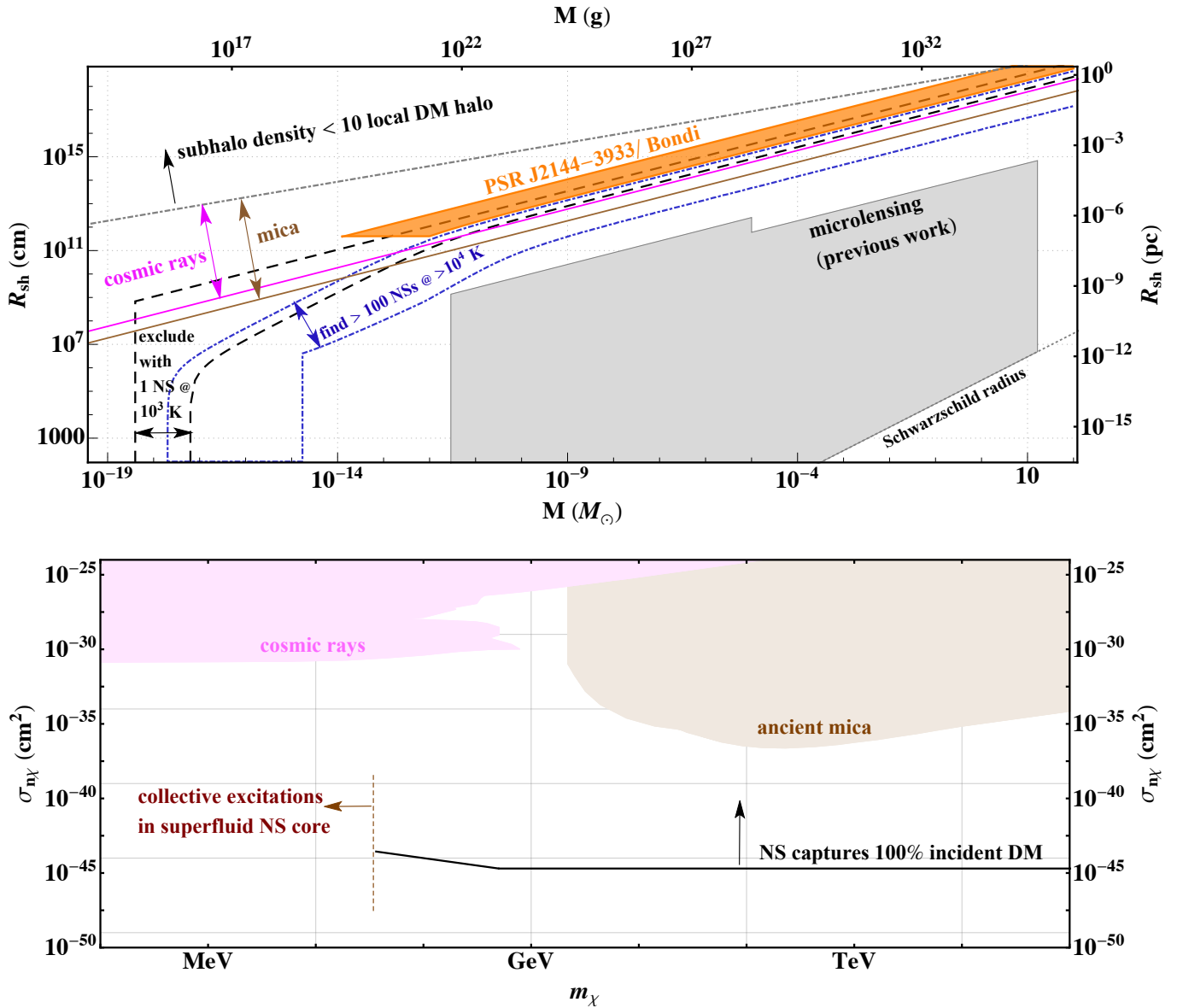


FIG. 2. Subhalo masses and radii probed by our detection strategies in the **top** panel, corresponding to limits on DM mass and nucleon scattering cross sections shown in the **bottom** panel. For collisionless DM, we show regions that can be probed by the observation of a single NS with 1000 K surface temperature (black dashed lines), as well as by future telescope surveys of NS within a kpc of Earth at the temperatures indicated (blue dot dashed lines). For dissipative/fluid DM, we exclude the orange region using observations of the coldest NS, for cross sections above the “100% capture” line in the bottom panel. Also shown are regions corresponding to existing constraints from DM-cosmic ray scattering (pink) and track searches in ancient mica (brown). Above the grey dot-dashed line, the galactic DM density exceeds the density in subhalos so DM does not significantly cluster. Limits from microlensing surveys are also shown. See text for more details.

ture. This condition is depicted in black in the bottom panel of Fig. 2, for velocity-independent elastic scattering, modeling the NS as a free fermion gas; in the region above the black curve all the DM flux incident on the NS is captured. As explained in Refs. [31, 83] and elsewhere, the mass capture rate is independent of  $m_\chi$ , hence the flat capture cross section for  $m_\chi \gtrsim 0.5$  GeV. Below this mass, Pauli-blocking of final state neutrons by the Fermi-degenerate nucleon medium reduces the capture

cross section in inverse proportion to  $m_\chi$ . Below  $m_\chi \simeq 35$  MeV the sensitivities require further study as there is a new effect: in a superfluid NS, DM cannot scatter elastically on nucleons, since the DM kinetic energy is insufficient to excite nucleons above the  $\mathcal{O}(\text{MeV})$  superfluid energy gap. In principle low-mass DM can still capture in NSs via excitation of collective modes such as phonons (see, e.g. Ref. [33]) and scattering with non-superfluid portions of the NS crust; we leave this to future work.

**Infrequent NS encounters.** For the scenario of  $t_{\text{meet}} > t_{\text{cool}}$  we cannot expect a steady-state temperature. Thus the strategy must be to look for NSs not long after encounter – corresponding to the right side of Fig. 1 – before they cool to temperatures below telescope sensitivities. This is done by surveying the sky for anomalously hot NSs.

In Fig. 2 top panel (again corresponding to the black capture region in the bottom panel) we show regions where at least 100 NSs with  $\tilde{T}_s > 10^4$  K are expected in the “solar vicinity,” defined as a kpc-radius circle around the Sun. Note that for the range of  $R_{\text{sh}}$  displayed, the subhalo crossing time is less than  $t_{\text{meet}}$ , where our treatment is valid. Currently, the HST is able to achieve point-source sensitivity as cold as  $3 \times 10^4$  K [52]. Similar directed observations of nearby pulsars with telescopes like LUVOIR [100] may provide an alternative strategy to find anomalously hot NSs. In addition, the observation of isolated  $> 10^3$  K NSs may be undertaken (see Supplementary Material) by the Roman/WFIRST survey [101] and in conjunction with deep-field observations by JWST, ELT and TMT [31]. We note that future optical survey sensitivities may detect  $10^4$  K NSs within  $\sim 20$  parsecs, as discussed in Supplementary Materials.

To obtain these regions we first estimate the probability of  $\tilde{T}_{\text{NS}}$  being at least some  $\tilde{T}_s$ , when heated by subhalo passage to a surface temperature  $\tilde{T}_s^{\text{hot}}$ , as

$$p(\tilde{T}_s^{\text{hot}} > \tilde{T}_{\text{NS}} > \tilde{T}_s) = 1 - e^{-t_s/t_{\text{meet}}} , \quad (11)$$

where  $t_s = t_{\text{cool}}(\tilde{T}_s) - t_{\text{cool}}(\tilde{T}_s^{\text{hot}})$  is the time taken for the NS to cool from  $\tilde{T}_s^{\text{hot}}$  to  $\tilde{T}_s$ . This expression accounts for Poisson probabilities for encounters and follows from the fact that  $p_1(\tilde{T}_s^{\text{hot}} > \tilde{T}_{\text{NS}} > \tilde{T}_s) = p_1(t_{\text{cool}}(\tilde{T}_s^{\text{hot}}) < t_{\text{cool}}(\tilde{T}_{\text{NS}}) < t_{\text{cool}}(\tilde{T}_s))$ ; a detailed derivation is provided in the Supplementary Material. We then multiply this probability with the number of NSs  $N_{\text{NS}}^{\odot}$  in the solar vicinity obtained from the NS surface density of Model 1A\* in Ref. [102]. This model assumes a Maxwell distribution of NS velocities consistent with our encounter rate, and gives  $N_{\text{NS}}^{\odot} \simeq 2 \times 10^5$ . As in Ref. [102] we assume that NSs are formed at a constant rate, so that the NS age distribution is peaked at the age of the Galaxy  $\simeq 5 \times 10^9$  yr.<sup>1</sup> This implies that the vast majority of the NSs we consider would have  $\tilde{T}_s \ll 1000$  K in the absence of subhalo heating (*cf.* the NS cooling curve in Fig. 1).

**Other probes.** COSMIC RAY SCATTERING. DM particles with stronger-than-electroweak cross sections would undergo appreciable scatters with Galactic CRs, which has been used to bound their scattering cross sections and masses by studying the subsequent softening of the CR spectrum [103], and by constraining the flux of gamma-rays [53] and up-scattered DM [54–57] produced in DM-CR collisions. These limits also apply to subhalo DM, as

the optical depth of CRs in the halo,  $\tau_{\text{CR}}$ , is unchanged from the case where DM is smooth. We verify this by computing  $\tau_{\text{CR}}$  for CRs contained in a diffusion zone of linear dimension  $L_{\text{dfs}}$  (about 1–15 kpc [104]) and subhalo number density  $n_{\chi} = \rho_{\chi}/M$  as

$$\tau_{\text{CR}} = \int_0^{L_{\text{dfs}}} ds n_{\chi}(s) \sigma_{\text{geo}} f_{\text{hit}} = \frac{\rho_{\odot}}{M} \sigma_{\text{geo}} f_{\text{hit}} D_{\text{eff}} , \quad (12)$$

where the geometric cross section of the subhalo and the number of CR scatters within a subhalo (for per-nucleus cross section  $\sigma_{N\chi}$ ) are given by

$$\sigma_{\text{geo}} = \pi R_{\text{sh}}^2 , \quad f_{\text{hit}} = \frac{\sigma_{N\chi}}{\pi R_{\text{sh}}^2} \frac{M}{m_{\chi}} . \quad (13)$$

In the top panel of Fig. 2, we show the  $M$ - $R_{\text{sh}}$  range constrained by CR scattering, for the  $\sigma_{N\chi}$ - $m_{\chi}$  range shown in the bottom panel. The top panel region is bounded from below by requiring that  $\tau_{\text{CR}} > 1$  (setting the effective diffusion length  $D_{\text{eff}} = 8.02$  kpc [54]). The upper bound is simply the requirement that DM is appreciably clustered in subhalos, quantified by the condition  $4\pi M/(3R_{\text{sh}}^3) > 10\rho_{\odot}$ .

PALEO-DETECTORS. Since they contain Gyr timescale archeological records of particle interactions, ancient mineral slabs are potentially sensitive to the historic passage of DM subhalos through the Earth. Decades ago, Refs. [58, 59] derived bounds on (unclumped) DM and monopole interactions by analyzing the microscopic structure of ancient mica; these constraints apply to subhalo DM as the total number of DM-mica scatters is unchanged by DM-clumping per an argument analogous to CR-scattering derived above. We thus show existing constraints in both panels of Fig. 2 similar to CR-scattering limits, with the  $R_{\text{sh}}$ - $M$  region now bounded on the right by the requirement that the timescale of Earth encounters with DM subhalos is smaller than the age of the mica samples (determined from fission track dating [59] to be  $(5 \pm 1) \times 10^8$  yr). Recently a number of proposals have suggested further mineralogic DM searches [72, 73, 105–108], including for subhalo DM [109].

In Fig. 2 we have also shown constraints from gravitational microlensing surveys [60, 61], with the reach in radii limited from below by each survey’s maximum Einstein radius, and reach in mass limited by observational cadences and finite source effects. While these constraints are agnostic to the scattering properties of DM, our probes are seen to highly complement them, reaching much larger and lighter subhalos. We have also indicated the Schwarzschild radii corresponding to large  $M$ ; the region below this line is unphysical. If a small fraction of DM remains unclumped, a possibility we have not explored in this study, direct detection searches may set bounds on the  $\sigma_{n\chi}$ - $m_{\chi}$  plane; on the other hand, our bounds on the plane apply for any distribution of DM into smooth and clumped components.

**Discussion.** This *Letter* charts the way forward for uncovering scattering interactions of subhalo DM. We

<sup>1</sup> We have verified that including a broader distribution of NS ages (as given in Ref. [102]) does not noticeably change our results.

have shown that cosmic ray scattering and mineral detection already provide some sensitivity, while novel methods using NS temperatures already constrain subhalo DM with strong self-interactions. In the future, subhalos over a vast range of masses and sizes may be uncovered by observations of either individual NSs or NSs in survey ensembles. Interestingly, imminent limits on the DM scattering cross section for subhalo-bound DM could become *stronger* than those from direct detection searches on unclumped DM (see Fig. 2 bottom panel and e.g., Ref. [110]).

Several new avenues await exploration. While DM could heat old NSs to detectable brightness by imparting kinetic energy, greater NS temperatures and other interesting signals could arise if DM annihilations in the NS core are present. For instance, if DM thermalizes slowly with the NS, annihilations may turn on late, so that there are two reheating periods in our “infrequent encounter” regime. DM annihilations following capture of subhalo DM could also produce detectable signals in a variety of celestial bodies [77, 111–113]. While we have focused on DM-nucleon scattering, some of our approaches also apply to DM that scatters on leptons. The lepton content of NSs, though relatively small, provides substantial sensitivity to DM-electron/muon scattering [47–51]. Up-scattering of DM with CR electrons should produce a detectable high-speed flux of DM, as with CR protons [55]. Exploring DM-electron scattering would therefore extend

our results to even lighter DM masses than depicted in Fig. 2. While for simplicity we had assumed uniform subhalo masses, more realistic mass distributions could be investigated.

Finally, our NS heating mechanism via DM subhalo encounters provides, in addition to probing the neutron portal to beyond-the-SM scenarios [114, 115], further motivation to imminent astronomical missions to make exciting discoveries in fundamental physics.

## ACKNOWLEDGMENTS

We thank Raghuvver Garani for discussions on neutron superfluidity. B.J.K. thanks the Spanish Agencia Estatal de Investigación (AEI, MICIU) for the support to the Unidad de Excelencia María de Maeztu Instituto de Física de Cantabria, ref. MDM-2017-0765. The work of J.B. and N.R. is supported by the Natural Sciences and Engineering Research Council of Canada. Research at Perimeter Institute is supported in part by the Government of Canada through the Department of Innovation, Science and Economic Development Canada and by the Province of Ontario through the Ministry of Colleges and Universities. TRIUMF receives federal funding via a contribution agreement with the National Research Council Canada.

- 
- [1] G. Bertone, D. Hooper, and J. Silk, *Phys. Rept.* **405**, 279 (2005), arXiv:hep-ph/0404175 [hep-ph].
  - [2] L. Baudis, *Phys. Dark Univ.* **4**, 50 (2014), arXiv:1408.4371 [astro-ph.IM].
  - [3] J. M. Gaskins, *Contemp. Phys.* **57**, 496 (2016), arXiv:1604.00014 [astro-ph.HE].
  - [4] M. Schumann, *J. Phys.* **G46**, 103003 (2019), arXiv:1903.03026 [astro-ph.CO].
  - [5] K. P. Zybin, M. I. Vysotsky, and A. V. Gurevich, *Phys. Lett. A* **260**, 262 (1999).
  - [6] S. Hofmann, D. J. Schwarz, and H. Stoecker, *Phys. Rev. D* **64**, 083507 (2001), arXiv:astro-ph/0104173.
  - [7] V. Berezhinsky, V. Dokuchaev, and Y. Eroshenko, *Phys. Rev. D* **77**, 083519 (2008), arXiv:0712.3499 [astro-ph].
  - [8] L. Bergstrom, J. Edsjo, P. Gondolo, and P. Ullio, *Phys. Rev. D* **59**, 043506 (1999), arXiv:astro-ph/9806072.
  - [9] F. C. van den Bosch, G. Ogiya, O. Hahn, and A. Burkert, *Mon. Not. Roy. Astron. Soc.* **474**, 3043 (2018), arXiv:1711.05276 [astro-ph.GA].
  - [10] F. C. van den Bosch and G. Ogiya, *Mon. Not. Roy. Astron. Soc.* **475**, 4066 (2018), arXiv:1801.05427 [astro-ph.GA].
  - [11] A. L. Erickcek and K. Sigurdson, *Phys. Rev. D* **84**, 083503 (2011).
  - [12] G. Barenboim and J. Rasero, *JHEP* **04**, 138 (2014), arXiv:1311.4034 [hep-ph].
  - [13] J. Fan, O. Özsoy, and S. Watson, *Phys. Rev. D* **90**, 043536 (2014).
  - [14] J. A. Dror, E. Kuflik, B. Melcher, and S. Watson, *Phys. Rev. D* **97**, 063524 (2018).
  - [15] P. W. Graham, J. Mardon, and S. Rajendran, *Phys. Rev. D* **93**, 103520 (2016).
  - [16] M. R. Buckley and A. DiFranzo, *Phys. Rev. Lett.* **120**, 051102 (2018), arXiv:1707.03829 [hep-ph].
  - [17] S. Nussinov and Y. Zhang, *JHEP* **03**, 133 (2020), arXiv:1807.00846 [hep-ph].
  - [18] G. Barenboim, N. Blinov, and A. Stebbins, (2021), arXiv:2107.10293 [astro-ph.CO].
  - [19] P. Gondolo and G. Gelmini, *Nucl. Phys.* **B360**, 145 (1991).
  - [20] N. Hiroshima, S. Ando, and T. Ishiyama, *Phys. Rev. D* **97**, 123002 (2018), arXiv:1803.07691 [astro-ph.CO].
  - [21] C. Blanco, M. S. Delos, A. L. Erickcek, and D. Hooper, *Phys. Rev. D* **100**, 103010 (2019), arXiv:1906.00010 [astro-ph.CO].
  - [22] M. Sten Delos, T. Linden, and A. L. Erickcek, *Phys. Rev. D* **100**, 123546 (2019), arXiv:1910.08553 [astro-ph.CO].
  - [23] M. S. Delos, *Phys. Rev. D* **100**, 063505 (2019), arXiv:1906.10690 [astro-ph.CO].
  - [24] K. Petraki and R. R. Volkas, *Int. J. Mod. Phys. A* **28**, 1330028 (2013), arXiv:1305.4939 [hep-ph].
  - [25] Y. Zhao, X.-J. Bi, H.-Y. Jia, P.-F. Yin, and F.-R. Zhu, *Phys. Rev. D* **93**, 083513 (2016), arXiv:1601.02181 [astro-ph.HE].
  - [26] Y. Zhao, X.-J. Bi, P.-F. Yin, and X. Zhang, *Phys. Rev. D* **97**, 063013 (2018), arXiv:1711.04696 [astro-ph.HE].

- [27] K. K. Boddy, J. Kumar, A. B. Pace, J. Runburg, and L. E. Strigari, *Phys. Rev. D* **102**, 023029 (2020), [arXiv:1909.13197 \[astro-ph.CO\]](#).
- [28] A. Drukier and L. Stodolsky, *Phys. Rev. D* **30**, 2295 (1984).
- [29] M. W. Goodman and E. Witten, *Phys. Rev. D* **31**, 3059 (1985).
- [30] A. K. Drukier, K. Freese, and D. N. Spergel, *Phys. Rev. D* **33**, 3495 (1986).
- [31] M. Baryakhtar, J. Bramante, S. W. Li, T. Linden, and N. Raj, *Phys. Rev. Lett.* **119**, 131801 (2017), [arXiv:1704.01577 \[hep-ph\]](#).
- [32] N. Raj, P. Tanedo, and H.-B. Yu, *Phys. Rev. D* **97**, 043006 (2018), [arXiv:1707.09442 \[hep-ph\]](#).
- [33] J. F. Acevedo, J. Bramante, R. K. Leane, and N. Raj, *JCAP* **03**, 038 (2020), [arXiv:1911.06334 \[hep-ph\]](#).
- [34] C.-S. Chen and Y.-H. Lin, *JHEP* **08**, 069 (2018), [arXiv:1804.03409 \[hep-ph\]](#).
- [35] N. F. Bell, G. Busoni, and S. Robles, *JCAP* **1809**, 018 (2018), [arXiv:1807.02840 \[hep-ph\]](#).
- [36] R. Garani, Y. Genolini, and T. Hambye, *JCAP* **1905**, 035 (2019), [arXiv:1812.08773 \[hep-ph\]](#).
- [37] D. A. Camargo, F. S. Queiroz, and R. Sturani, *JCAP* **1909**, 051 (2019), [arXiv:1901.05474 \[hep-ph\]](#).
- [38] K. Hamaguchi, N. Nagata, and K. Yanagi, *Phys. Lett. B* **795**, 484 (2019), [arXiv:1905.02991 \[hep-ph\]](#).
- [39] W.-Y. Keung, D. Marfatia, and P.-Y. Tseng, *JHEP* **07**, 181 (2020), [arXiv:2001.09140 \[hep-ph\]](#).
- [40] N. F. Bell, G. Busoni, S. Robles, and M. Virgato, (2020), [arXiv:2004.14888 \[hep-ph\]](#).
- [41] B. Dasgupta, A. Gupta, and A. Ray, *JCAP* **10**, 023 (2020), [arXiv:2006.10773 \[hep-ph\]](#).
- [42] R. Garani, A. Gupta, and N. Raj, *Phys. Rev. D* **103**, 043019 (2021), [arXiv:2009.10728 \[hep-ph\]](#).
- [43] T. N. Maity and F. S. Queiroz, (2021), [arXiv:2104.02700 \[hep-ph\]](#).
- [44] N. F. Bell, G. Busoni, T. F. Motta, S. Robles, A. W. Thomas, and M. Virgato, (2020), [arXiv:2012.08918 \[hep-ph\]](#).
- [45] Y.-P. Zeng, X. Xiao, and W. Wang, (2021), [arXiv:2108.11381 \[hep-ph\]](#).
- [46] F. Anzuini, N. F. Bell, G. Busoni, T. F. Motta, S. Robles, A. W. Thomas, and M. Virgato, (2021), [arXiv:2108.02525 \[hep-ph\]](#).
- [47] N. F. Bell, G. Busoni, and S. Robles, *JCAP* **1906**, 054 (2019), [arXiv:1904.09803 \[hep-ph\]](#).
- [48] R. Garani and J. Heeck, *Phys. Rev. D* **100**, 035039 (2019), [arXiv:1906.10145 \[hep-ph\]](#).
- [49] A. Joglekar, N. Raj, P. Tanedo, and H.-B. Yu, (2019), [arXiv:1911.13293 \[hep-ph\]](#).
- [50] A. Joglekar, N. Raj, P. Tanedo, and H.-B. Yu, (2020), [arXiv:2004.09539 \[hep-ph\]](#).
- [51] N. F. Bell, G. Busoni, S. Robles, and M. Virgato, *JCAP* **03**, 086 (2021), [arXiv:2010.13257 \[hep-ph\]](#).
- [52] S. Guillot, G. G. Pavlov, C. Reyes, A. Reisenegger, L. Rodriguez, B. Rangelov, and O. Kargaltsev, *Astrophys. J.* **874**, 175 (2019), [arXiv:1901.07998 \[astro-ph.HE\]](#).
- [53] R. H. Cyburt, B. D. Fields, V. Pavlidou, and B. D. Wandelt, *Phys. Rev. D* **65**, 123503 (2002), [arXiv:astro-ph/0203240](#).
- [54] T. Bringmann and M. Pospelov, *Phys. Rev. Lett.* **122**, 171801 (2019), [arXiv:1810.10543 \[hep-ph\]](#).
- [55] Y. Ema, F. Sala, and R. Sato, *Phys. Rev. Lett.* **122**, 181802 (2019), [arXiv:1811.00520 \[hep-ph\]](#).
- [56] C. Cappiello and J. F. Beacom, *Phys. Rev. D* **100**, 103011 (2019), [arXiv:1906.11283 \[hep-ph\]](#).
- [57] M. Andriamirado *et al.* (PROSPECT), (2021), [arXiv:2104.11219 \[hep-ex\]](#).
- [58] P. Price and M. Salamon, *Phys. Rev. Lett.* **56**, 1226 (1986).
- [59] D. Snowden-Ifft, E. Freeman, and P. Price, *Phys. Rev. Lett.* **74**, 4133 (1995).
- [60] D. Croon, D. McKeen, and N. Raj, *Phys. Rev. D* **101**, 083013 (2020), [arXiv:2002.08962 \[astro-ph.CO\]](#).
- [61] D. Croon, D. McKeen, N. Raj, and Z. Wang, *Phys. Rev. D* **102**, 083021 (2020), [arXiv:2007.12697 \[astro-ph.CO\]](#).
- [62] J. A. Dror, H. Ramani, T. Trickle, and K. M. Zurek, *Phys. Rev. D* **100**, 023003 (2019), [arXiv:1901.04490 \[astro-ph.CO\]](#).
- [63] Y. Bai, A. J. Long, and S. Lu, *JCAP* **09**, 044 (2020), [arXiv:2003.13182 \[astro-ph.CO\]](#).
- [64] J. Bramante, B. Broerman, R. F. Lang, and N. Raj, *Phys. Rev. D* **98**, 083516 (2018), [arXiv:1803.08044 \[hep-ph\]](#).
- [65] J. Bramante, B. Broerman, J. Kumar, R. F. Lang, M. Pospelov, and N. Raj, *Phys. Rev. D* **99**, 083010 (2019), [arXiv:1812.09325 \[hep-ph\]](#).
- [66] J. Bramante, J. Kumar, and N. Raj, *Phys. Rev. D* **100**, 123016 (2019), [arXiv:1910.05380 \[hep-ph\]](#).
- [67] J. F. Acevedo, J. Bramante, A. Goodman, J. Kopp, and T. Opferkuch, *JCAP* **04**, 026 (2021), [arXiv:2012.09176 \[hep-ph\]](#).
- [68] J. F. Acevedo, J. Bramante, and A. Goodman, *Phys. Rev. D* **103**, 123022 (2021), [arXiv:2012.10998 \[hep-ph\]](#).
- [69] P. Adhikari *et al.*, (2021), [arXiv:2108.09405 \[astro-ph.CO\]](#).
- [70] J. F. Acevedo, J. Bramante, and A. Goodman, (2021), [arXiv:2108.10889 \[hep-ph\]](#).
- [71] D. M. Jacobs, G. D. Starkman, and B. W. Lynn, *Mon. Not. Roy. Astron. Soc.* **450**, 3418 (2015), [arXiv:1410.2236 \[astro-ph.CO\]](#).
- [72] R. Ebadi *et al.*, *Phys. Rev. D* **104**, 015041 (2021), [arXiv:2105.03998 \[hep-ph\]](#).
- [73] J. F. Acevedo, J. Bramante, and A. Goodman, (2021), [arXiv:2105.06473 \[hep-ph\]](#).
- [74] A. Das, S. A. R. Ellis, P. C. Schuster, and K. Zhou, (2021), [arXiv:2106.09033 \[hep-ph\]](#).
- [75] D. Stiff, L. M. Widrow, and J. Frieman, *Phys. Rev. D* **64**, 083516 (2001), [arXiv:astro-ph/0106048](#).
- [76] M. Kamionkowski and S. M. Koushiappas, *Phys. Rev. D* **77**, 103509 (2008), [arXiv:0801.3269 \[astro-ph\]](#).
- [77] A. Ibarra, B. J. Kavanagh, and A. Rappelt, *JCAP* **12**, 013 (2019), [arXiv:1908.00747 \[hep-ph\]](#).
- [78] J. I. Collar, *Phys. Lett. B* **368**, 266 (1996), [arXiv:astro-ph/9512054](#).
- [79] B. J. Kavanagh, T. D. P. Edwards, L. Visinelli, and C. Weniger, (2020), [arXiv:2011.05377 \[astro-ph.GA\]](#).
- [80] T. D. P. Edwards, B. J. Kavanagh, L. Visinelli, and C. Weniger, (2020), [arXiv:2011.05378 \[hep-ph\]](#).
- [81] J. Binney and S. Tremaine, *Galactic Dynamics: Second Edition*, by James Binney and Scott Tremaine. ISBN 978-0-691-13026-2 (HB). Published by Princeton University Press, Princeton, NJ USA, 2008. (Princeton University Press, 2008).
- [82] A.-C. Eilers, D. W. Hogg, H.-W. Rix, and M. K. Ness, *The Astrophysical Journal* **871**, 120 (2019).

- [83] I. Goldman and S. Nussinov, *Phys. Rev.* **D40**, 3221 (1989).
- [84] H. Bondi and F. Hoyle, *Mon. Not. Roy. Astron. Soc.* **104**, 273 (1944).
- [85] H. Bondi, *Mon. Not. Roy. Astron. Soc.* **112**, 195 (1952).
- [86] M. C. Begelman, *Mon. Not. Roy. Astron. Soc.* **181**, 347 (1977).
- [87] E. Shima, T. Matsuda, H. Takeda, and K. Sawada, *Mon. Not. Roy. Astron. Soc.* **217**, 367 (1985).
- [88] D. G. Yakovlev, K. P. Levenfish, and Y. A. Shibano, *Phys. Usp.* **42**, 737 (1999), arXiv:astro-ph/9906456.
- [89] D. Page and S. Reddy, *Ann. Rev. Nucl. Part. Sci.* **56**, 327 (2006), arXiv:astro-ph/0608360.
- [90] B. Haskell and A. Sedrakian, *Astrophys. Space Sci. Libr.* **457**, 401 (2018), arXiv:1709.10340 [astro-ph.HE].
- [91] A. Y. Potekhin, D. A. Zyuzin, D. G. Yakovlev, M. V. Beznogov, and Y. A. Shibano, *Mon. Not. Roy. Astron. Soc.* **496**, 5052 (2020), arXiv:2006.15004 [astro-ph.HE].
- [92] D. D. Ofengeim, M. Fortin, P. Haensel, D. G. Yakovlev, and J. L. Zdunik, *Phys. Rev. D* **96**, 043002 (2017), arXiv:1708.08272 [astro-ph.HE].
- [93] D. D. Ofengeim and D. G. Yakovlev, *Mon. Not. Roy. Astron. Soc.* **467**, 3598 (2017).
- [94] J. H. Chang, D. Egana-Ugrinovic, R. Essig, and C. Kouvaris, *JCAP* **03**, 036 (2019), arXiv:1812.07000 [hep-ph].
- [95] R. Huo, H.-B. Yu, and Y.-M. Zhong, *JCAP* **06**, 051 (2020), arXiv:1912.06757 [astro-ph.CO].
- [96] J. Liu, X.-P. Wang, and W. Xue, *Phys. Rev. D* **100**, 123012 (2019), arXiv:1902.02348 [hep-ph].
- [97] X. Shen, P. F. Hopkins, L. Necib, F. Jiang, M. Boylan-Kolchin, and A. Wetzel, (2021), 10.1093/mnras/stab2042, arXiv:2102.09580 [astro-ph.GA].
- [98] M. Ryan, J. Gurian, S. Shandera, and D. Jeong, (2021), arXiv:2106.13245 [astro-ph.CO].
- [99] S. Tulin and H.-B. Yu, *Phys. Rept.* **730**, 1 (2018), arXiv:1705.02358 [hep-ph].
- [100] LUVUOIR, (2019), arXiv:1912.06219 [astro-ph.IM].
- [101] WFIRST, (2012), arXiv:1208.4012 [astro-ph.IM].
- [102] N. Sartore, E. Ripamonti, A. Treves, and R. Turolla, *Astronomy and Astrophysics* **510**, A23 (2010).
- [103] C. V. Cappiello, K. C. Y. Ng, and J. F. Beacom, *Phys. Rev. D* **99**, 063004 (2019), arXiv:1810.07705 [hep-ph].
- [104] T. Bringmann, F. Donato, and R. A. Lineros, *JCAP* **01**, 049 (2012), arXiv:1106.4821 [astro-ph.GA].
- [105] A. K. Drukier, S. Baum, K. Freese, M. Górski, and P. Stengel, *Phys. Rev. D* **99**, 043014 (2019), arXiv:1811.06844 [astro-ph.CO].
- [106] T. D. P. Edwards, B. J. Kavanagh, C. Weniger, S. Baum, A. K. Drukier, K. Freese, M. Górski, and P. Stengel, *Phys. Rev. D* **99**, 043541 (2019), arXiv:1811.10549 [hep-ph].
- [107] S. Baum, A. K. Drukier, K. Freese, M. Górski, and P. Stengel, *Phys. Lett. B* **803**, 135325 (2020), arXiv:1806.05991 [astro-ph.CO].
- [108] S. Baum, T. D. P. Edwards, B. J. Kavanagh, P. Stengel, A. K. Drukier, K. Freese, M. Górski, and C. Weniger, *Phys. Rev. D* **101**, 103017 (2020), arXiv:1906.05800 [astro-ph.GA].
- [109] S. Baum, W. DeRocco, T. D. P. Edwards, and S. Kalia, (2021), arXiv:2107.02812 [astro-ph.GA].
- [110] Y. Meng *et al.* (PandaX-4T), (2021), arXiv:2107.13438 [hep-ex].
- [111] R. K. Leane and J. Smirnov, *Phys. Rev. Lett.* **126**, 161101 (2021), arXiv:2010.00015 [hep-ph].
- [112] R. K. Leane, T. Linden, P. Mukhopadhyay, and N. Toro, *Phys. Rev. D* **103**, 075030 (2021), arXiv:2101.12213 [astro-ph.HE].
- [113] R. K. Leane and T. Linden, (2021), arXiv:2104.02068 [astro-ph.HE].
- [114] D. McKeen, M. Pospelov, and N. Raj, *Phys. Rev. D* **103**, 115002 (2021), arXiv:2012.09865 [hep-ph].
- [115] D. McKeen, M. Pospelov, and N. Raj, *Phys. Rev. Lett.* **127**, 061805 (2021), arXiv:2105.09951 [hep-ph].
- [116] A. Cumming, E. F. Brown, F. J. Fattoyev, C. J. Horowitz, D. Page, and S. Reddy, *Phys. Rev. C* **95**, 025806 (2017), arXiv:1608.07532 [astro-ph.HE].
- [117] D. Page, J. M. Lattimer, M. Prakash, and A. W. Steiner, *Astrophys. J. Suppl.* **155**, 623 (2004), arXiv:astro-ph/0403657 [astro-ph].
- [118] D. G. Yakovlev and C. J. Pethick, *Ann. Rev. Astron. Astrophys.* **42**, 169 (2004), arXiv:astro-ph/0402143 [astro-ph].
- [119] E. H. Gudmundsson, C. J. Pethick, and R. I. Epstein, *Astrophys. J.* **272**, 286 (1983).
- [120] M. V. Beznogov, A. Y. Potekhin, and D. G. Yakovlev, *Phys. Rept.* **919**, 1 (2021), arXiv:2103.12422 [astro-ph.SR].
- [121] H. T. Diehl and et al., (2019), 10.2172/1596042.
- [122] J. R. Peterson, (2016), 10.2172/1272167.
- [123] v. Ivezić *et al.* (LSST), *Astrophys. J.* **873**, 111 (2019), arXiv:0805.2366 [astro-ph].
- [124] R. E. Rutledge, D. B. Fox, M. Bogosavljevic, and A. Mahabal, *Astrophys. J.* **598**, 458 (2003), arXiv:astro-ph/0302107.
- [125] M. L. Turner, R. E. Rutledge, R. Letcavage, A. S. H. Shevchuk, and D. B. Fox, *Astrophys. J.* **714**, 1424 (2010), arXiv:1003.3955 [astro-ph.HE].
- [126] W. Voges *et al.*, *Astron. Astrophys.* **349**, 389 (1999), arXiv:astro-ph/9909315.
- [127] P. Predehl *et al.*, *Astron. Astrophys.* **647**, A1 (2021), arXiv:2010.03477 [astro-ph.HE].



# SUPPLEMENTARY MATERIAL

## I. PASSIVE COOLING TIME

In this section we provide some physics background to Eq. (10). We first recall that temperatures denoted with a tilde are in the frame of a distant observer. During quiescent periods the NS temperature evolution is given by

$$c_\nu(\tilde{T}) \frac{d\tilde{T}}{dt} = -L_\nu^\infty(\tilde{T}) - L_\gamma^\infty(\tilde{T}), \quad (14)$$

where the neutrino luminosity of the NS as measured by a distant observer of our benchmark NS is given by [116]

$$L_\nu^\infty(\tilde{T}) = 1.33 \times 10^{39} \text{ J/yr} \left( \frac{\tilde{T}}{10^9 \text{ K}} \right)^8, \quad (15)$$

applicable for slow/modified Urca processes, which we take to be the only neutrino cooling mechanism as prescribed by the ‘‘minimal cooling’’ paradigm [117]. These processes dominate the NS cooling down to  $\tilde{T} = 10^8 \text{ K}$  before photon cooling takes over. The luminosity of photon blackbody emission from the NS surface is:

$$L_\gamma^\infty(\tilde{T}_s) = 4\pi(1+z)^2 R_{\text{NS}}^2 \tilde{T}_s^4. \quad (16)$$

To solve Eq. (14) we need a relation between  $T_s$  and  $T$ , which depends on the composition of the outermost envelope, which acts as an insulating layer for temperatures above  $\mathcal{O}(10^3) \text{ K}$ . For smaller temperatures the envelope becomes too thin for insulation, and the surface temperature reflects the internal temperature [91, 118]. We assume a standard iron envelope for which we have the following relation at high temperatures [119, 120]:

$$T_s = 10^6 \text{ K} \left[ \left( \frac{M_{\text{NS}}}{1.5 M_\odot} \right) \cdot \left( \frac{10 \text{ km}}{R_{\text{NS}}} \right)^2 \right]^{1/4} \left[ \frac{T}{9.43 \times 10^7 \text{ K}} \right]^{0.55}. \quad (17)$$

We identify the thin-envelope regime by solving for  $T_s = T$  in the above equation, giving  $T_{\text{env}} = 3908 \text{ K}$ . Below this temperature we model the  $T_s - T$  relation by simply setting  $T_s = T$ .

We now have all the ingredients to solve Eq. (14). We do this by following the prescription in Ref. [93], suitably improving it to account for the thin-envelope  $T_s - T$  relation, and obtain the analytic solution in Eq. (10).

## II. PROBABILITIES OF OBSERVING HEATED NEUTRON STARS

The probability of observing an NS above some temperature  $\tilde{T}_s$ , as given in Eq. (11), is derived as follows.

Consider first  $p_i(\tilde{T} > \tilde{T}_s)$ , the probability that at the end of  $i$  encounters the NS temperature  $\tilde{T}$  at the time

of observation exceeds some threshold  $\tilde{T}_s$ . (We implicitly assume here that  $\tilde{T}_{\text{hot}} > \tilde{T}_s$ .) We then note that  $p_i(\tilde{T} > \tilde{T}_s) = p_i(t < t_s)$ , where  $t$  is the time between the  $i$ th encounter and the observation (i.e. the time since the last encounter) and  $t_s$  is the time taken to cool from  $\tilde{T}_{\text{hot}}$  to  $\tilde{T}_s$ . That is, if the most recent encounter occurred a time  $t < t_s$  ago, then the NS temperature will still exceed  $\tilde{T}_s$ .

If there are exactly  $i$  encounters over a time  $t_{\text{NS}}$ , then

$$\begin{aligned} p_i(t < t_s) &= 1 - p_i(t > t_s) \\ &= 1 - p_i(N_{[t_{\text{NS}} - t_s, t_{\text{NS}}]} = 0) \\ &= 1 - \left( 1 - \frac{t_s}{t_{\text{NS}}} \right)^i, \end{aligned} \quad (18)$$

where  $N_{[t_{\text{NS}} - t_s, t_{\text{NS}}]}$  is the number of encounters which occur in a time interval between  $[t_{\text{NS}} - t_s, t_{\text{NS}}]$ . The second term in the second line of Eq. (18) is therefore the probability of having no encounters within a time  $t_s$  before the observation of the NS. This is then evaluated explicitly in the next line by noting that the Poisson-distributed encounters occur uniformly over the time interval  $t \in [0, t_{\text{NS}}]$ .

The expected number of encounters in a time  $t_{\text{NS}}$  is  $\lambda = t_{\text{NS}}/t_{\text{meet}}$ , hence the Poisson probability  $p_{\text{meet},i}$  of having  $i$  encounters is

$$p_{\text{meet},i} = \frac{\lambda^i e^{-\lambda}}{i!}. \quad (19)$$

Accounting for multiple encounters, and using Eqs. (18) and (19), we obtain the required probability in Eq. (11) as

$$\begin{aligned} p(\tilde{T} > \tilde{T}_s) &= \sum_{i \geq 1} p_{\text{meet},i} p_i(t < t_s) \\ &= \sum_{i \geq 1} \frac{\lambda^i e^{-\lambda}}{i!} \left[ 1 - \left( 1 - \frac{t_s}{t_{\text{NS}}} \right)^i \right] \\ &= 1 - e^{-t_s/t_{\text{meet}}}. \end{aligned} \quad (20)$$

Here we have included only terms with  $i \geq 1$  because we assume that the equilibrium NS temperature exceeds  $\tilde{T}_s$ , so at least one encounter is required to be detectable. Note that the above expression holds for all  $t_s$  and  $t_{\text{meet}}$ . In particular, for  $t_s \ll t_{\text{meet}}$ , the exponential in Eq. (20) tends to zero and we end up with  $p(\tilde{T} > \tilde{T}_s) \rightarrow 1$ , as expected in the frequent encounter regime.

## III. MORE TARGET REGIONS FOR FUTURE TELESCOPES

In Fig. 3 we show regions further to those shown in Fig. 2 that could be probed by future telescopes. We see that the triangular region corresponding to observing a single NS at or below  $10^4 \text{ K}$  is consistent with Fig. 1. We

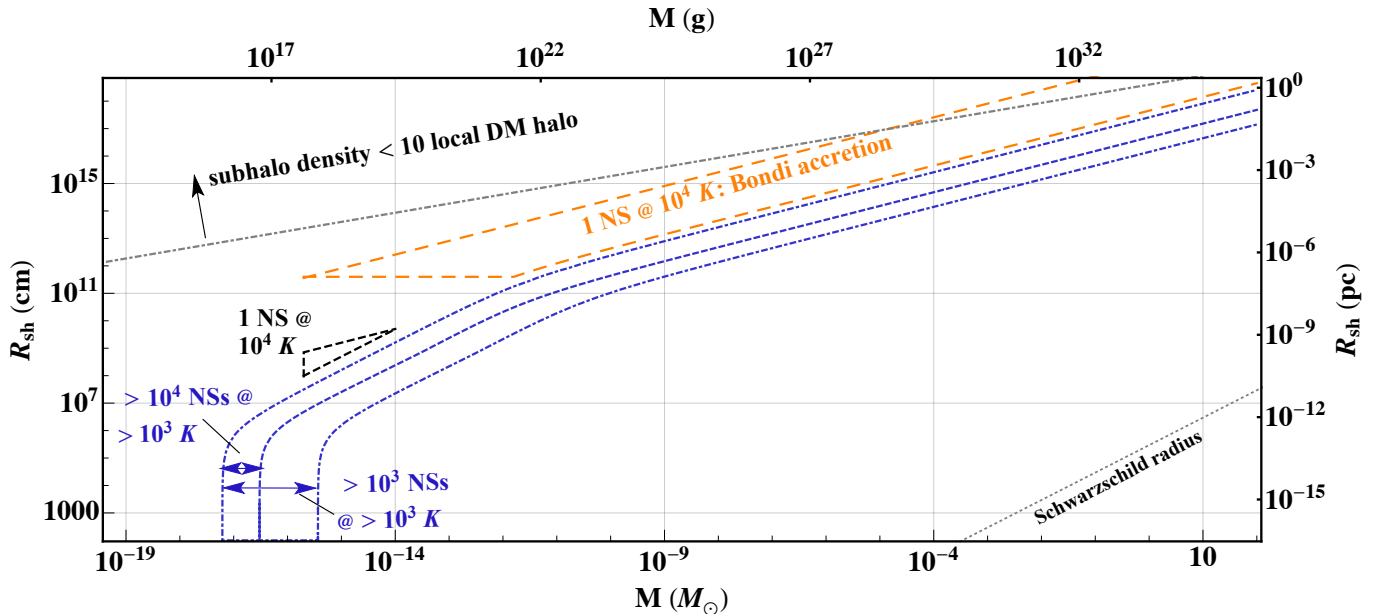


FIG. 3. Same as the top panel of Figure 2, but showing the regions that may be constrained by observing (1) a single NS below  $10^4$  K; also shown is the region that may be probed if Bondi accretion of self-interacting subhalos is present, (2) at least  $10^3$  and  $10^4$  NSs below  $10^3$  K in an infrared survey.

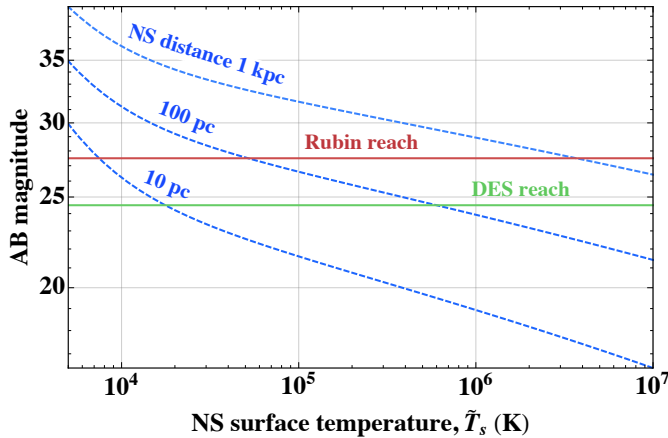


FIG. 4. The g-band AB magnitude point source sensitivity of the deep field Dark Energy Survey and the projected Rubin sensitivity, compared to the luminosity of a neutron star with distances from Earth and surface temperatures indicated. Recall that larger magnitudes correspond to fainter objects.

also see that in the presence of Bondi accretion (for subhalos with dissipative self-interactions), due to a larger collection radius than for collisionless DM (Eq. (4)), a much larger  $M$ - $R_{\text{sh}}$  region may be probed for  $R_{\text{sh}}$  exceeding the Bondi radius.

In the coming decades, astronomical surveys have interesting prospects for the discovery of subhalo-heated NSs. In Fig. 4 we show the sensitivity of optical surveys

alongside the luminosity of nearby NSs. The Dark Energy Survey [121] and the planned Rubin/LSST [122, 123] achieve g-band AB magnitude sensitivities of 24.5 and 27.5, compared with a fainter 31 AB magnitude for a  $10^4$  K NS at a distance of 0.1 kpc. We see that it may be possible for Rubin to discover or exclude the existence of subhalo-heated NSs within tens of parsecs from Earth. This would provide some information on whether the Earth is located inside or near a subhalo.

Finally, for the sake of completeness we make a few comments about x-ray survey sensitivity to subhalo-heated NSs. Using the ROSAT all-sky survey as well as infrared and radio source maps, limits have been set on the number of x-ray emitting NSs near the solar position [124, 125]. The ROSAT flux count sensitivity of  $5 \times 10^{-13} \text{ cm}^{-2} \text{ s}^{-1}$  in the 0.1–2.4 keV band corresponds to an AB magnitude sensitivity of 25–28, which has permitted the discovery of  $\gtrsim 5 \times 10^5$  K NSs within  $\sim 0.5$  kpc [126]. At present, ROSAT results limit the number of nearby x-ray emitting isolated NSs to less than 48 at 90% C.L. [125]. The upcoming eRosita all-sky survey is expected to improve on the flux sensitivity by a factor of 25 [127]. However, we find that the NS temperatures required for x-ray detection of NSs ( $\gtrsim 10^5$  K) lie well above temperatures that would be imparted by subhalo DM near the solar position. Nevertheless, in future studies it would be interesting to explore the subhalo DM sensitivity that would be provided by x-ray searches for NSs near the Galactic Center, where DM densities are higher.